UV Autofluorescence Microscopy of Dinosaur Bone Reveals Encapsulation of Blood Clots within Vessel Canals

Mark H. Armitage* and Jim Solliday
DSTRI, Inc., 325 East Washington Street #170, Sequim, WA 98382
*micromark@juno.com

Abstract: Remarkable discoveries such as condensed chromatin in duckbill dinosaur cartilage and newly presented discoveries of dinosaur vascular veins, venule valves, and nerve fibers (this report) warrant study of global dinosaur remains for preserved soft tissue (dST). Dinosaur osteocytes feature dendritic projections (filipodia) of lengths up to 18 µm, while osteocytes collected from a *Triceratops* horn have lengths of 25 µm or longer. While preservation methods for dST involve the degradation of sugars into glycation end products and the employment of highly oxidative hydroxyl radicals to "fix" tissues, we note that lengthy and narrow osteocyte filipodia show no signs of hydroxyl radical infiltration into the lacuna-canalicular network. Moreover, our ultraviolet fluorescence (UVFL) study of *Triceratops* horn, rib, vertebra, and frill thin sections shows extensive clotting in most vessel canals, probably as a result of asphyxia while drowning. Further UVFL autofluorescence study of dinosaur bone sections is vital for characterization of dinosaur blood clots.

Keywords: dinosaur, soft tissue, blood clots, tissue preservation, autofluorescence

Introduction

Dinosaur remains, especially fossil bone, continue to reveal exceptionally preserved dinosaur soft tissues (dST) including endogenous osteocytes, chondrocytes, intact vessels, collagen, and other soft tissues that have been widely reported from dinosaur compact bone fossils [1–8]. Recently, condensed chromatin within chondrocyte nuclei undergoing chondroptosis-mimicking cellular metaphase was reported from duckbill dinosaur fossil material recovered in the late 1980s at the Two Medicine Formation in Montana [3]. Another study of 19 museum bone specimens, including 15 dinosaur bones, selected from the paleontology collection at the University of Alberta, showed that all specimens yielded soft tissues [9]. These striking discoveries, from specimens collected decades ago (3 in the case of the condensed chromatin specimen) provide strong justification for ongoing examination of dinosaur bones for dST.

Dinosaur blood vessels have been described and analyzed at length [5–7,10,11], but dinosaurian veins, with characteristic venous valves, have not been reported. It would not be surprising to find veins and venous valves along with dinosaur osteocytes, blood vessels, and even intact nerves, post decalcification. Here we present new findings of these novel dinosaur soft tissue structures; venous valves, veins, and nerve fibers, from *Triceratops horridus* bone specimens (HCTH-02, 03, horn, HCTR-11 rib, and HCTV-22 vertebra) collected previously [1] (Figures 1–6). These tissue elements were liberated simultaneously and are shown here, suggesting that dinosaur neurovascular bundles travel as a triad of veins, vessels, and nerve fibers, as in other vertebrates [12].

Microscopic venous valves (Figures 1–3) in humans are well characterized in the literature [13–16]. They ensure that blood flow continues to move forward (with each heart pulse) as blood flows to the heart. Valves in human dermis are 25 µm or less in diameter, and the thin leaflets (cuspids) that make up the (usually) bicuspid valves are typically 1 µm thick [15]. Transmission electron microscopy (TEM) has shown that valve leaflets are delicate membranes of connective tissue (elastin and collagen) with layers of endothelial cells lining each leaflet. These thin cuspids of venule valves prevent backflow, therefore it is reasonable to expect that postmortem blood would be held in direct contact with venule valves for extended periods of time after death. Pooling at such sites via gravitational settling into dependent or lower portions of the body begins within 20 minutes of death and is characterized by clotting and permanence after 7 hours [17]. Blood might also pool in place in the veins and vessels of bone. Over time, if blood cells lyse, iron is freed from the hemoglobin and generates copious amounts of hydroxyl radicals, which would be expected to damage ultrathin valve cuspids (see Soft Tissue Preservation Methods below). We observed no damage to cuspids in this study; in fact, we observed standing vein valves that retained aqueous solutions via closed cuspids that trapped bacteria (unpublished data).

Veins were usually flattened and delicate, averaging 20–55 µm in diameter (Figure 4). Although clumps of very small veins that autofluoresced brightly under blue light were observed, most veins were elongated and flattened. Vein branching patterns and branching angles were observable even though the three-dimensional conformation of these elements was flattened by liberation from the bone.

Nerves recovered from *T. horridus* (HCTV-22, Figures 5–6) exhibited birefringence in polarized light [18,19]. Polarized light examination of extant vertebrate nerves reveals an undulating or zig-zagging sub-structure called "*Bands of Fontana*," a feature characteristic of vertebrate nerves [18,20]. These white bands are also seen in the dinosaur nerve fiber on the right side of Figure 6 (arrows).

Dinosaur Bone Cells

Dinosaur osteocytes have been broadly reported, whether liberated into solution or observed on surfaces of partially decalcified compact bone, as being anchored by distinctive filipodia, which are the long dendritic processes characteristic of bone cells [1,2,5–9,11,21,22]. Most bone cells reside in crystalline bone matrix where they are trapped during early bone growth and remodeling. They create a broad arrangement of three-dimensional connections via the extension of

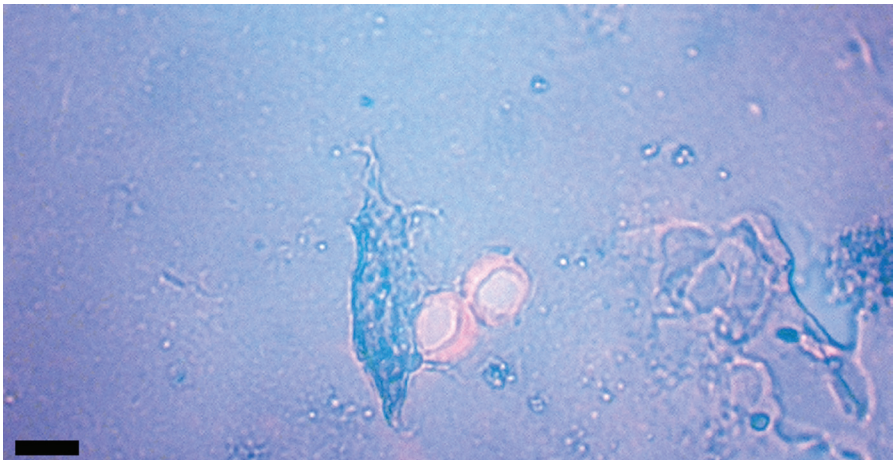

Figure 1: Venule valves from HCTH-02 (see Methods) liberated with EDTA. Valves are stained with acridine orange for nucleic acid detection. Scale bar, 50 µm.

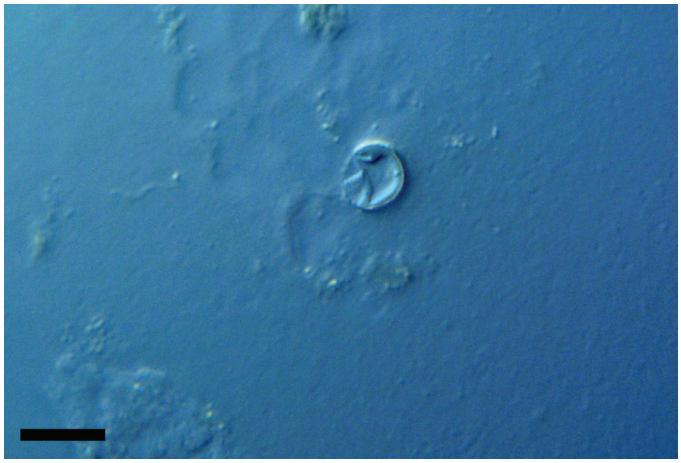

Figure 2: Valve with folded leaflets visible (differential interference contrast [DIC] microscopy). Scale bar, 50 µm.

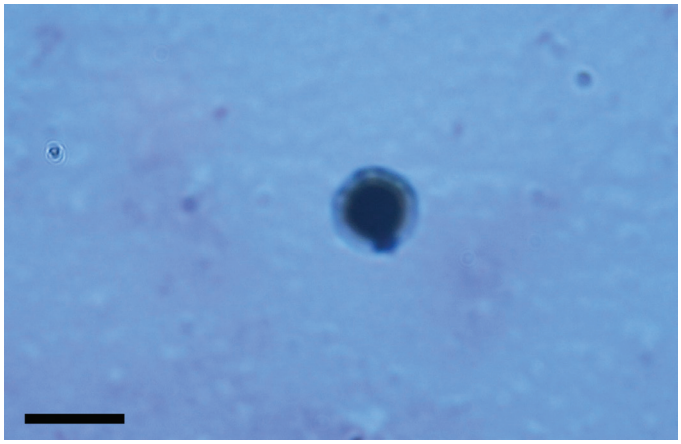

Figure 3: Valve with leaflets heavily stained with toluidine blue tissue stain. Scale bar, 50 µm.

their processes throughout bone tunnels known as canaliculi. Dendritic processes travel from bone lacunae (the indentations that cells lie within) through fluid-filled canaliculi to reach other cells. There they connect using gap junctions. Workers note that in humans "the average cumulated length of a single cell process projecting from an osteocyte cell body including all its sub-branches is 47 µm" [23]. They also estimate that osteocytes have upwards of 89 dendritic processes per cell. Dinosaur osteocytes show similar numbers of extensions protruding from the cell membrane (Figure 7), but lengths over 18 µm have not been reported.

Attention has been drawn to "extended" dinosaur filipodial length [5–8]. Descriptions such as "long filipodia," "long extensive filipodia," "long flexible filipodia," "very long extensive filipodia," and "extensive three-dimensional filipodial network" are used to describe intact filipodia [5–7]. In some instances, where dinosaur osteocytes have been reported, image scale bars are not present or are obscured [8,24], but for the most part scales are supplied. Most cells feature non-cumulated filipodia lengths under 15–16 µm. One notable exception is that cells recovered from *B. canadensis* filipodia show filipodia lengths up to 18 µm [8,22], but lengths of 47 µm are unreported for dinosaur bone cell dendrites. Nevertheless, it is clear that many dST osteocytes characterized to date (especially those liberated from bone matrix) are marked by truncated or completely missing filipodia [5,7,8,21]. Dinosaur osteocytes with filipodia longer than 18 µm seem rare.

This rarity might result from any number of variables, including initial degradation of cells within bone before processing, attachment of filipodia to inner canaliculi walls, rough handling during processing, lengthy exposure to decalcification reagents, and desiccation or improper dehydration. In other words, processing artifacts and unforeseen degradation prior to processing can disrupt cellular architecture. Additionally, prior to processing environmental extremes such as freeze/thaw cycles, heat and desiccation exposure, exposure to naturally occurring radioactive decay, water or mud infiltration, ingress of soil microbes, bacteria, worms, insects, plant roots, fungal hyphae, and the like all result in cell degradation. Moreover, natural events that occur *within cells* immediately postmortem would certainly affect dendritic length. Schweitzer has remarked, "The preservation of cells is difficult to account for in the fossil record, as autolytic destruction of cells and intracellular contents may begin within seconds after death" [22].

Widths of osteocyte filipodia are noted at 200 nm in humans [25], but widths of dinosaur osteocytes are rarely reported [1]. Human canaliculi width radii have been estimated at 157.5 nm [23], thus the filipodia traversing these tunnels would be thinner to fit comfortably. This conforms to measurements on dinosaur osteocyte filopodia in this study. With lengths extending some 125 times their diminutive widths, they might well be characterized as the most delicate among soft tissue elements found within dinosaur bones. Therefore, it is reasonable to expect that they would be susceptible to degradation as a result of any foreign intrusions into the lacuno-canalicular network.

Fossil osteocytes of *Triceratops* horn from Hell Creek, Montana (HCTH-02) show filipodia of 25 µm in length under

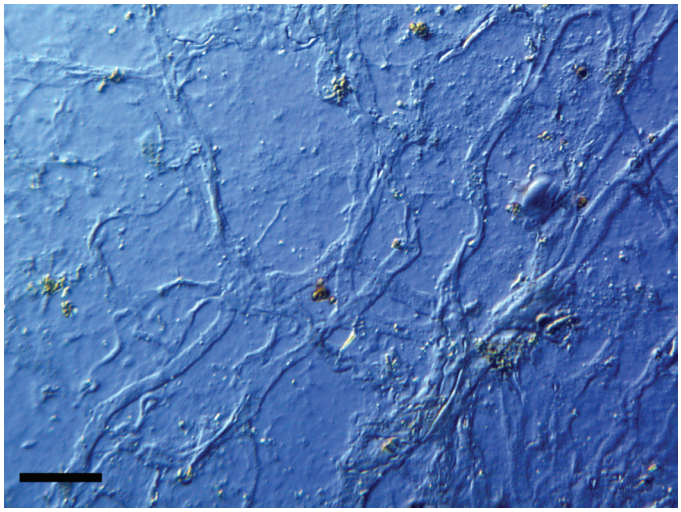

Figure 4: Intact veins from HCTH-02 (DIC microscopy). Scale bar, 40 µm.

scanning electron microscopy (SEM) (Figure 7, left side, arrows) especially when imaged as uncoated specimens. We predict that with more deliberate methods, bone cells with longer dendrites will be liberated from dinosaur bone.

Soft Tissue Preservation Mechanisms

It was once thought that bacterial biofilms mimicked the morphology of dST, however those claims have been eliminated [11]. Armitage [26] cryo-thin sectioned sheets of fibrillar bone after mechanically peeling them from exposed horncore (*T. horridus* HCTH-02). Frozen sections (9 µm thickness) revealed rows of embedded osteocytes stacked three-dimensionally on each other. It is impossible for biofilms to replicate three-dimensionally stacked (and filipodia-linked) cells.

Presently two complimentary systems of preservation are proposed to account for the survival of endogenous blood vessels through deep time. The first of these has been described as transition metal-catalyzed intermolecular crosslinking [6,11], which will be reviewed shortly. The second complementary preservation process is based on the natural degradation that takes place when reducing sugars decay to advanced glycation end products over time. This mechanism cannot guarantee preservation of labile tissues, but it may add resistance to degradation and microbial decomposition of endogenous proteins over time [3,10].

With respect to metal-catalyzed crosslinking of vessels, transition metals are necessary for protein stabilization. Free iron (heme) is normally bound up by intracellular proteins in large quantities within tissues and cells. Cells mediate cytotoxicity by binding heme with specialized proteins [27]. Heme is also very highly concentrated within erythrocytes [28]. It is proposed by some workers that heme (or hemoglobin from red blood cells) is liberated post-mortem and acts to generate hydroxyl radicals (Fenton reactions), which "fix" tissues similar to the way aldehydes fix tissue for microscopy [10,11]. Hydroxyl (HO) and peroxyl (HOO) radicals are said to stabilize collagen and elastin structural proteins via crosslink formation, particularly within vessel wall amino acids [10]. The added stability might confer stiffness and harden resistance to degradation of vessels over deep time.

Hemoglobin is clearly the stated source for iron mediated stabilization of dST [11] as there is an "intimate association" between iron particles and soft tissues, particularly bone cells (see section Ultraviolet Fluorescence and Autofluorescence of Bone). "Blood cells rich in iron-containing HB flow through vessels and have access to bone osteocytes through the lacuna-canalicular network," [11]. What is not explained is how hemoglobin trapped in erythrocytes avoids the inescapable blood cascade reaction known as thrombosis, which initiates clot production immediately upon tissue injury or body trauma [29]. In response to tissue damage, prothrombin in the blood becomes activated to thrombin. Thrombin rapidly cleaves fibrinogen into fibrin fibers. Deposition of fibrin fibers (along with the expression of a host of co-factors) into the blood vessels activates the clotting cascade. Fibrin segments form a meshwork of fibers upon which the rest of the clot is assembled, particularly after platelets are activated to assist in clot formation. Erythrocytes are captured and sequestered within clots adding rigidity. Thrombin production continues and peaks within about 6 minutes after injury in a "burst" eruption [30,31]. This lasts as long as platelets and co-factors are plentiful in plasma and on cells to maintain the reaction, but in less than 30 minutes clot formation enters a stability phase [31].

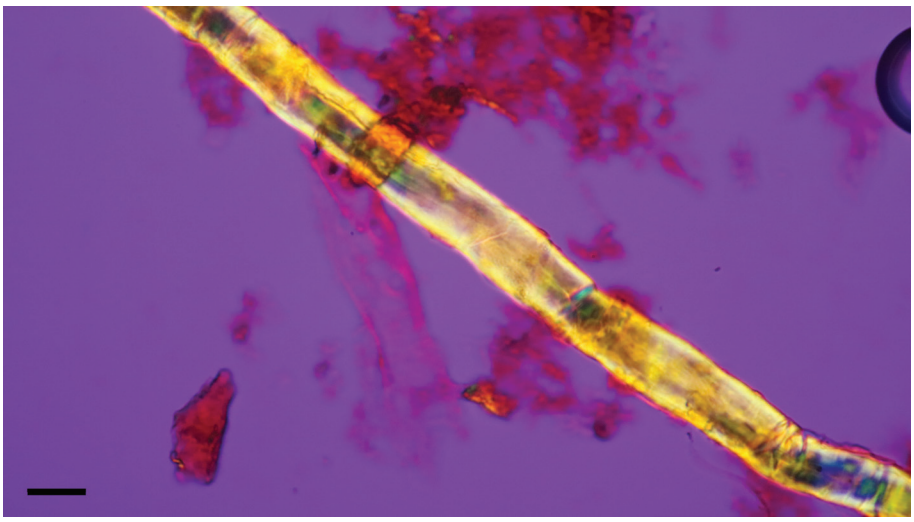

Figure 5: Intact neural filament from HCTV-22 showing birefringence under polarized light with a ¼ wave plate. Scale bar, 40 µm.

Intriguingly, it has been shown that when whole blood is exposed to metal-catalyzed oxidizing reagents, fibrinogen can be modified by hydroxyl radicals thus inhibiting thrombin-induced clot formation [31]. However, it has not been determined how thrombosis, once activated, might influence the production of hydroxyl radicals in dinosaur tissues or inhibit the passage of free water through vessels, which is required for Fenton reaction longevity. For Fenton hydroxyls to reach, envelop, and preserve tissues deeply sequestered in bone, several requirements must be met; RBCs

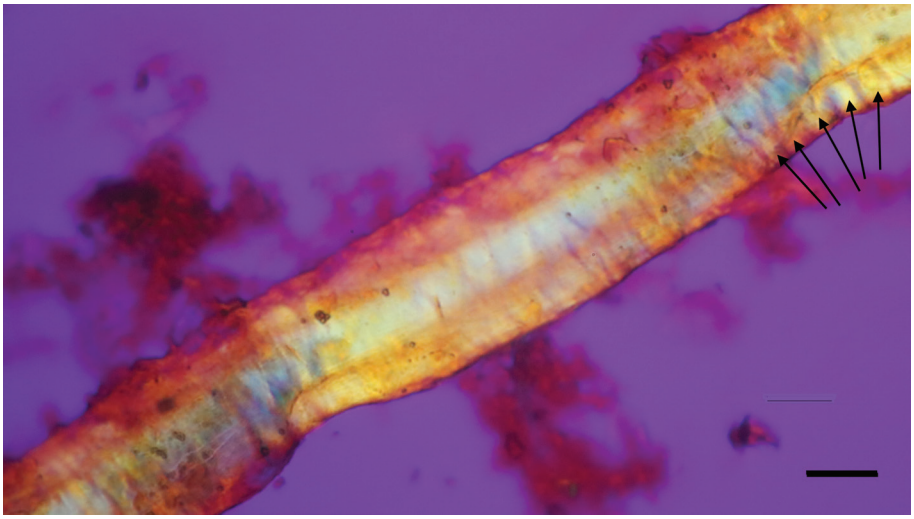

Figure 6: Higher magnification from Figure 5 showing undulating white *Bands of Fontana* (arrows). Scale bar, 20 µm.

must be lysed, hemoglobin must be released (and degraded), and oxygen and water must be present to generate hydroxyls.

The highly reactive hydroxyl (HO) and peroxyl (HOO) species generated during Fenton chemistry are known to be highly destructive to biomolecules [27,28,32–36]. McCord [34] has stated, "This hydroxyl radical can attack all classes of biological macromolecules. It can depolymerize polysaccharides, cause DNA strand breaks, inactivate enzymes and initiate lipid peroxidation … lipid peroxidation is a chain reaction … ". Hawkins and Davies [32] note that it can be frustrating to determine the sites of radical attack on large proteins because of the chain-reaction attacking nature of the radicals; "Some of these reactions are chain processes, with a greater concentration of amino acids damaged than initial attacking radicals generated," and "15 amino acids [are] consumed per HO generated which is modest by comparison with lipid peroxidation." Balla et al. [28] found that iron-derived reactive oxygen species are responsible for "numerous vascular disorders," and are highly toxic to cells because of "the ease with which this highly hydrophobic compound can enter and cross cell membranes," leaving oxidized, damaged, and dead cells.

Other workers add, "DNA, proteins, lipids and other organics are damaged and destroyed by oxidative radicals" [35]. Schaer et al. [37] have remarked, "When hemoglobin (Hb) bursts from RBCs because of hemolysis, the naked Hb, devoid of its antioxidant sentries that are normally available within the RBC, can wreak oxidative havoc in the vasculature and in exposed tissues." They add, " … Hb and hemin (oxidized heme) trigger vascular and organ dysfunction that leads to adverse clinical effects." Loures et al. [33] list the reduction potential of hydroxyl radicals as second only to fluorine and show they are 30% more reactive than peroxyl radicals.

Thus, it is well established that Fenton reactions can be highly destructive to cells, tissues, and proteins. This high reactivity, and in theory ability of free iron to destroy cell membranes, should destroy more tissues than it helps. However, in the case of the *Triceratops* horn collected from the Hell Creek Formation, filipodia from bone osteocytes imaged *just outside* of the vessel canals are long and unfragmented (Figure 7, see arrows), suggesting that Fenton reactions never occurred within the lacuno-canalicular network of the horn and thus never acted on cell membranes or filipodial extensions.

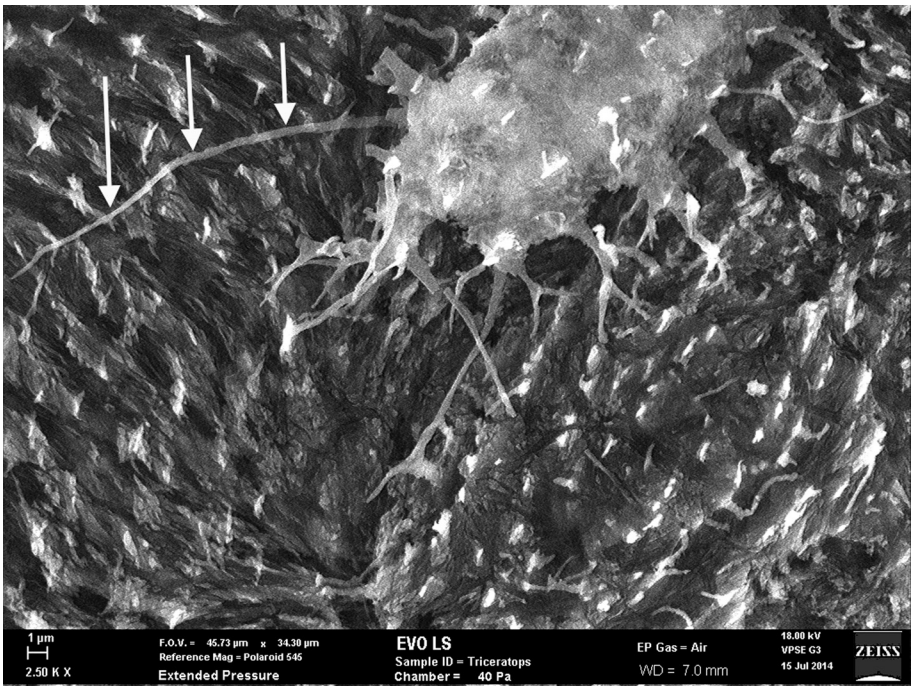

Figure 7: SEM of uncoated *Triceratops* horn (HCTH-03) osteocyte with 24 µm long filipodia (arrows, left side). Scale bar, 1 µm.

What of Clotting?

Schweitzer et al. took extraordinary measures to inhibit thrombosis during experiments conducted on ostrich vessels soaked in hemoglobin [11]. Chicken and ostrich blood collected for the harvesting of heme was infused with anticoagulant (EDTA) upon collection. It was subsequently centrifuged at high rpm and later filtered to separate plasma, serum, cells (white cells and platelets), cell debris (after red blood cells were mechanically lysed), and all associated tissue factors and co-clotting factors that initiate and regulate the normal thrombotic reaction. A more rigorous experimental investigation would benefit by real-world conditions of buried animal remains.

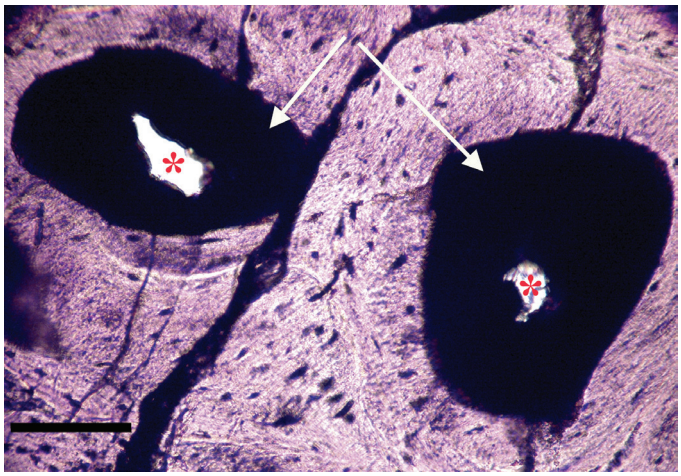

Figure 8a: Ground section, *Triceratops* vertebra (HCTV-22). Haversian canals are almost completely blocked by a dark amorphous material (arrows). Asterisks indicate small openings within clots. Light microscopy, brightfield. Scale bar, 100 µm.

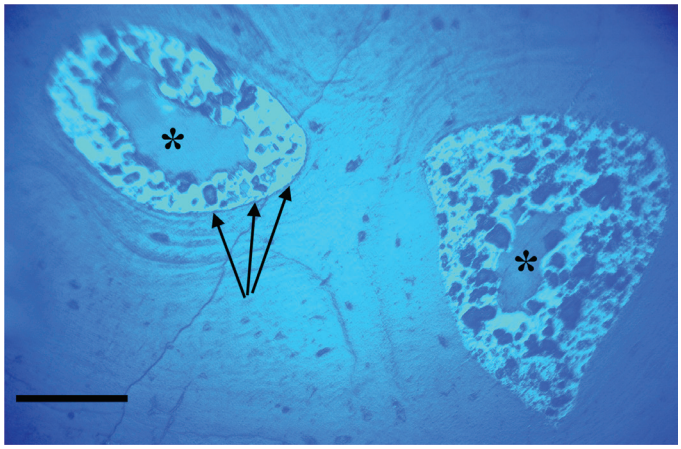

Figure 8b: Same view under UV epi-fluorescence (UVFL). Clots are marked by a brightly reflective layer (BRL) with internal opaque chunks, which completely fill the vessel canal and abut closely to vessel canal walls. Asterisks indicate small openings within the clots. Clots are characterized by sharp margins (dense line, black arrows), and do not spread into adjacent bone. Scale bar, 100 µm.

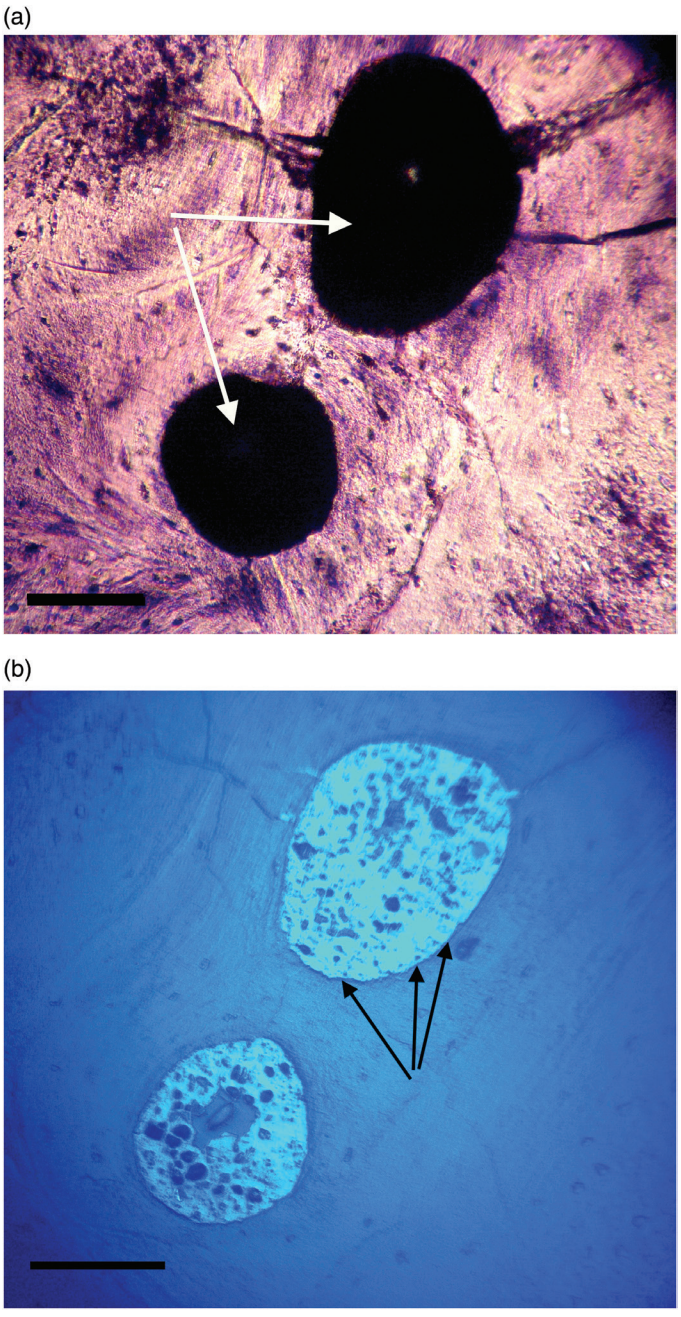

Figure 9a, 9b: *Triceratops* horn (HCTH-03). Canals are completely clotted. Under UV (9b), a brightly reflective homogenous layer encases and surrounds darker crystallized shards, probably crystallized blood products. These darker shards are never found outside of the brightly reflective material and are usually characterized as highly angular particles under 20 µm in width, although many are rounded (see white arrows, Figure 11b). Scale bar, 100 µm.

Later, workers incubated specimens of chicken bone microvasculature in ferrous chloride (instead of hemoglobin) to initiate non-enzymatic crosslinks in vessel collagen and elastin [10]. Any potential problems associated with the presence of real-world thrombin, prothrombin, fibrinogen, fibrin, cell and tissue factors, etc. were eliminated. Vessel sections were examined, post-treatment, by SR-FTIR, and signs of increased intramolecular crosslinking of structural proteins were observed. These were compared with similar crosslinks found in untreated, sectioned dinosaur vessels. Boatman et al. conclude, "Exposure of extant chicken type I collagen tissues to Fenton chemistry and transition metal-catalyzed glycation rapidly induces chemical modifications observed in the dinosaur tissues studied here … these molecular features confer resistance to degradation in tissues that possess them…" [10].

As mentioned, thrombosis is often initiated within the vasculature of animals as a response to trauma including major tissue or head (brain or cranial) injury and most particularly in drowning cases [38,39]. Trauma-related disseminated intravascular coagulation (DIC) occurs when fibrinogen is cleaved into fibrin (as above) and deposited systemically into the vasculature, forming microvascular clots throughout the body [40]. DIC might also be exacerbated by an underlying disorder that triggers and then maintains coagulation in the microvasculature [41]. Studies also

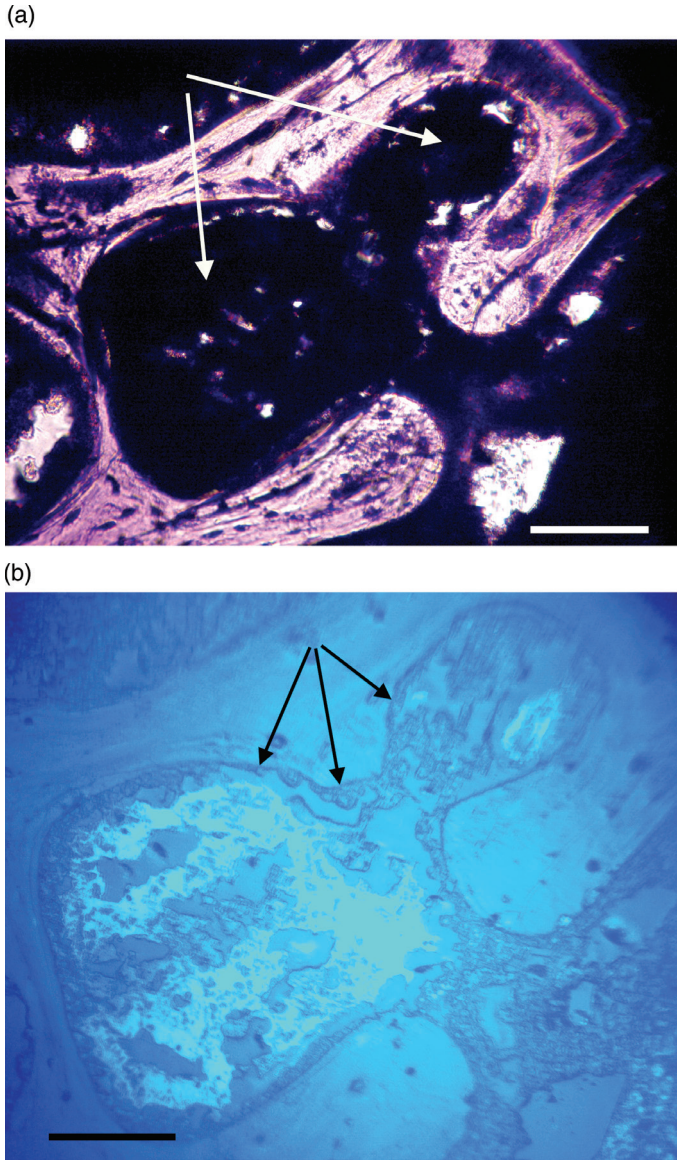

Figure 10a, 10b: *Triceratops* rib (HCTR-11). Clots in Haversian canals and an anastomosing canal (right of center). Some clearings are visible, but canals are mostly occluded. Under UV (10b), rib clots were not as organized as in horn and vertebra, and the brightly reflective layer is somewhat diffuse, less organized, and not abutted to canal walls. Scale bar, 100 µm.

show that acute mental stress can elevate hemoconcentration, plasma viscosity, lipid concentrations, and certain tissue clotting factors [42,43]. If enough platelets and clotting factors are available, the clotting cascade will be maintained until resources are exhausted, but cellular death will interrupt the cascade. If death is averted, and as platelets are depleted, DIC can reverse, and systemic, untreatable bleeding might occur [39]. This is observed only in a low number of cases [40]. Interestingly, autopsy findings of human patients with overt DIC exhibited systemic clots throughout all small, medium, and large arteries and veins [40,41].

In the case of *Triceratops* animals buried at Hell Creek, trauma and asphyxiation are suggested as the cause of death based on the specific fluvial architectural elements found there [44]. The Hell Creek Formation in Glendive, MT (and surrounding areas) has been characterized as a low coastal plain with meandering fluvial systems with occasional catastrophic flooding resulting in some extinction [44,45]. If *Triceratops* in the Hell Creek Formation drowned while suffering major tissue injury in a flooding event, the microvasculature within bones might be characterized by heavy clotting. This clotting could have inhibited the passage of water (required to maintain ongoing Fenton reactions) and could have sequestered free iron in RBCs within clots making it unavailable for the generation of hydroxyls and peroxyls.

In this study we examined ground sections of *Triceratops* bone for evidence of clotting and sequestration of iron in microvascular canals.

Methods

Triceratops bones, including horn (HCTH-02, 03), rib (HCTR-11), and vertebra (HCTV-22) previously collected within the Hell Creek Formation in Montana [1] were processed for ground thin sections of 80 µm thickness. *Triceratops* frill (HCTF-39), collected at the same location in 2015, was similarly processed. Microvascular canals were examined on non-coverslipped sections under a UV-fluorescence (Hund, Wetzlar Germany H500) microscope supplied with a 100 W mercury burner. Specimens were excited at UV wavelengths (254 nm, 366 nm), and autofluorescence images were captured with a ProgRes CF-cool (Jenoptik, Germany) low-light camera.

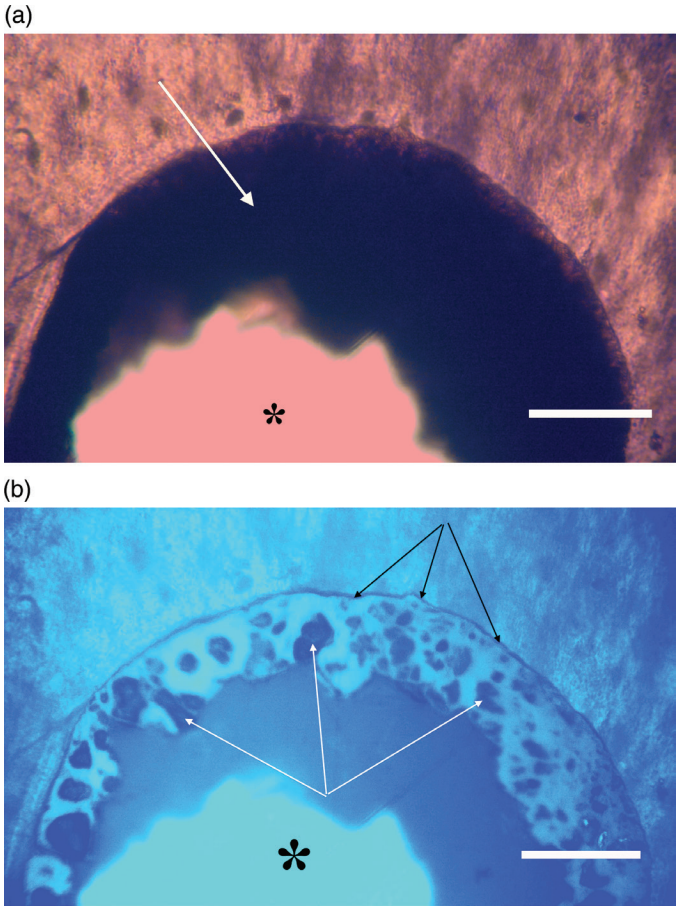

Figure 11a, 11b: *Triceratops* frill (HCTF-39). Clot with large central opening (asterisks). Note distinct outer dark margin line of clot, appressed to canal wall (black arrows, 11b). White arrows point to angular shards embedded within brightly reflective layer. Scale bar, 100 µm.

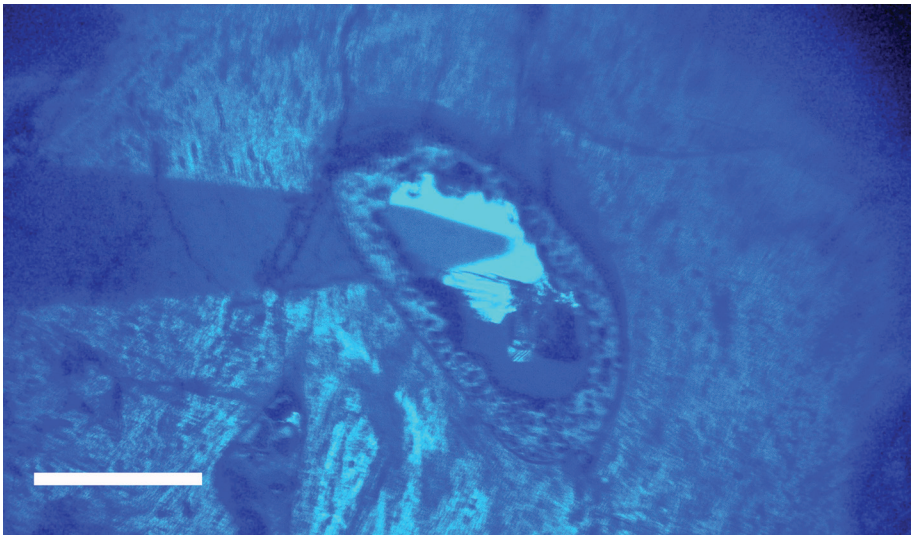

Figure 12: *Triceratops* frill. A steel pin placed on the surface of the field diaphragm is imaged clearly through a fluorescing clot opening demonstrating that neither the embedding polymer nor the ground surface is autofluorescing. Scale bar, 100 µm.

Results

All *Triceratops* ground sections exhibited heavy clotting in all vessel channels except those that were closest to the bone edge, a processing artifact. These mature bones were typical; presenting newly formed Haversian systems as well as older, partially resorbed ones. Irregular interstitial areas were also observed, as were the concentric lamellae encircling canals. Fine radiating canaliculi and lacunae were apparent.

Most microvascular channels, particularly those under 200 µm in width, were completely obstructed by clots (Figures 8–10, white arrows). Some had small openings within the clots (Figures 8a, 8b, 11b, asterisks). These clear openings were situated near lumen centers in canals. Partial clearing of canals could mean that clots might have been restricted to short lengths in veins, possibly a result of deep vein thrombosis in settings of low shear flow such as at venule-cuspid junctions [46]. Alternately clots may have been dislodged, perforated, or lost during processing, creating openings. Angular crystalline structures, light brown and somewhat translucent in nature (Figures 8a and 11a), are clearly seen in the open spaces within clots. These were observed in every vessel canal. Clots exhibited a dense, narrow outer marginal layer (black arrows Figures 8b, 9b, 10b, 11b), and clot material never crossed over this margin into compact bone, remaining isolated in canals.

Ultraviolet Fluorescence and Autofluorescence of Bone

Autofluorescence is an intrinsic property of some biological compounds (especially within cells and tissues) that receive and are excited by energy, such as light energy. When energy is transferred the compounds fluoresce or give off light energy as the influx of excitation energy stabilizes [47,48]. Many biological molecules and structures such as collagen, elastin, flavins, porphyrins, and pyroxidines autofluoresce in response to UV illumination.

Ultraviolet fluorescence microscopy (UVFL) is a useful tool for imaging specific features of bone, which autofluoresces under certain conditions, and has had widespread medical use [49–54]. UVFL examination of dinosaur bone is rare with only a few studies of UVFL application to dinosaur specimens including examination of dinosaur fossil feathers [55] and bones of birds related to dinosaurs [57]. However, these did not utilize autofluorescence microscopy. UVFL autofluorescence microscopy (and fluorophore-based microscopy) of dinosaur bone thin sections represents a unique opportunity to study well-preserved tissue and cellular morphology of dST *in situ*.

In order to generate autofluorescence, high levels of light energy with a broad-based spectrum are directed at specimens being examined. The emission spectrum of the 100 W mercury burner used in this study provides high irradiance between 275–500 nm [56]. This would certainly supply enough excitation energy to elicit responses from iron along several of its emission lines including 374.55 nm even if bound in clots. That line has the highest autofluorescence emission intensity for Fe I [58], however 26 other strong emission lines have been reported for Fe I and II between 234.34 nm and 400 nm [58]. Clots imaged here emitted light between 375 and 450 nm, thus emission falls within the expected range of autofluorescence wavelengths for Fe I and Fe II.

It could be argued that the brightly reflective layer is just an artifact of grinding during processing. To test this possibility, the point of a pin at 100×, placed just at the sub-stage field diaphragm of the microscope, using low intensity transmitted light, was optically resolved while focusing through an opening in the center of an autofluorescing clot (Figure 12). If the embedding polymer was autofluorescing, or if a grinding artifact might be creating a roughened surface that might otherwise be autofluorescing, the point of the pin (13 cm below the specimen) would be obscured or unresolved. Moreover, the clot completely obscures the pin shaft in Figure 12, yet the pin shaft is visible through the bone mineral, thus the clot is denser than the bone itself.

Discussion and Conclusions

This report of blood clots in dinosaur bones is controversial, much as reports of other blood related products has been [4–7]. Nevertheless, although tentative, observations presented here warrant further investigation into the nature of dinosaur blood clots, especially the concentrations and oxidation state of iron in them. Iron response to UV light is significant and shows up as a brightly reflective bluish-white layer with embedded angular objects (Figures 8b, 9b, 10b, 11b, 12). We conclude that the non-fluorescing angular objects are crystallized blood products within each vessel occlusion. It is unlikely that the brightly reflective layer and the angular crystals within them represent an unconsolidated influx of soil matrix deep into frill and horn bone specimens because the emission from the brightly reflective layer is uniform over all sections studied and is only disturbed by embedded

crystals which uniformly do not autofluoresce. On the other hand, UVFL of mixed sediment and clay grains could present as a non-uniform and markedly different set of fluorescent responses within each "clot."

Many soil minerals and clay particles are known to autofluoresce and can cause a strong background soil autofluorescence signal. This can interfere with other fluorescent biomaterials [59,60]. All clots in this study had a similar, uniform appearance except for the rib sections, where in some instances there was less cohesion across the clot. The rib clots also appeared less brightly reflective. However, if these "clots" represent sediment grains which were deeply infiltrated into the microvasculature they would react differently to high-emission UV wavelengths and would not look as uniform as seen here. We conclude these are the remains of blood products that clotted, possibly during drowning or another traumatic event.

The literature on dST lacks discussion of blood clots, rigor mortis and livor mortis, and any possible effects on the specific set of requirements needed for profitable Fenton reactions to occur. We conclude here that free iron was unavailable, at least in these *Triceratops* bones, because clotted vessels would have blocked water from flowing over lysed RBCs.

Other questions that remain to be answered include:

- Are the intermittent vessel structural protein crosslinks suggested by Bailleul et al. [3] sufficient to stabilize vessels over deep time, even if the tissues are somewhat sequestered by mineral encrustation?
- What of the stability of the amino acids in the proteins that are *not* crosslinked by Fenton hydroxyl actions? What keeps them from dissociating over time?
- Why have there been no studies of the other amino acids from these structural proteins, which would serve as markers for hydroxyl exposure (for example, see DeMassa and Boudreaux, [61])?
- How do observations of clotted microvasculature explain the presence of osteocytes with long filipodia, nerve bundles, vein valves, or condensed chromosomes [3]?

References

[1] MH Armitage and KL Anderson, *Acta Histochemica* 115 (2013) 603–08.
[2] MH Armitage, *Microscopy Today* 24 (2016) 18–22.
[3] AM Bailleul et al., *Nat Sci Rev* 7 (2020) 815–22.
[4] MH Schweitzer and JR Horner, *Ann Paleontol* 85 (1999) 179–92.
[5] MH Schweitzer et al., *Science* 307 (2005) 1952–55.
[6] MH Schweitzer et al., *Proc Roy Soc B* 274 (2007) 183–97.
[7] MH Schweitzer et al., *Science* 324 (2009) 626–31.
[8] MH Schweitzer et al., *Bone* 52 (2013) 414–23.
[9] AJ Van der Reest and PJ Currie, *Cretaceous Res* 109 (2020) 1–11.
[10] EM Boatman et al., *Sci Rep* 9 (2019) 15678–89.
[11] MH Schweitzer et al., *Proc Roy Soc B* 281 (2013) 20132741. Suppl. info: http://dx.doi.org/10.1098/rspb.2013.2741.
[12] WR Porter and LM Witmer, *Anat Rec* 303 (2019) 1075–1103.
[13] IM Braverman and A Keh-Yen, *J Invest Derm* 77 (1981) 297–304.
[14] IM Braverman and A Keh-Yen, *J Invest Derm* 81 (1983) 438–42.
[15] A Caggiati et al., *Eur J Vasc Endovasc Surg* 32 (2006) 447–52.
[16] S Takase et al., *J Vasc Surg* 39 (2004) 1329–34.
[17] A Rayamane et al., *J Forensic Med Toxicol* 31 (2014) 12–17.
[18] J Cha et al., *Biomed Opt Exp* 9 (2018) 1097–1110.
[19] KWTK Chin et al., *Biomed Opt Exp* 8 (2017) 4122–34.
[20] C Stolinski, *J Anat* 186 (Pt 1) (1995) 123–30.
[21] MH Schweitzer et al., *Comptes Rendus Palevol* 7 (2008) 159–84.
[22] MH Schweitzer, *Ann Rev Earth Planet Sci* 39 (2011) 187–216.
[23] PR Buenzli and NA Sims, *Bone* 75 (2015) 144–50.
[24] MH Schweitzer, *Scientific American* 303 (2010) 62–69.
[25] A Mogilner and B Rubenstein *Biophys J* 89 (2005) 782–95.
[26] MH Armitage, *American Laboratory* 40 (March 2012) cover.
[27] J Balla et al., *Antiox Redox Sig* 9 (2007) 2119–38.
[28] J Balla et al., *Mol Nutrition Food Res* 49 (2005) 1030–43.
[29] A Satyam et al., *Acute Med Surg* 6 (2019) 329–35.
[30] AS Wolberg, *Blood Rev* 21 (2007) 131–42.
[31] AS Wolberg and RA Campbell, *Transfusion Apheresis Sci* 38 (2008) 15–23.
[32] CL Hawkins and MJ Davies, *Biochim Biophys Acta* 1504 (2001) 196–219.
[33] CCA Loures et al., *Int Rev Chem Eng* 5(2013) 102–20.
[34] JM McCord, *Semin Hematol* 35 (1998) 5–12.
[35] S Park and JA Imlay, *J Bact* 185 (2003) 1942–50.
[36] J Prousek, *Pure Appl Chem* 79 (2007) 2325–38.
[37] DJ Schaer et al., *Blood* 121 (2013) 1276–84.
[38] M Levi and H ten Cate, *New Engl J Med* 341 (1999) 586–92.
[39] M Schwameis et al., *Crit Care Med* 43 (2015) 2394–2402.
[40] M Levi, *Brit J Haemat* 124 (2004) 567–76.
[41] M Levi, *Crit Care Med* 35 (2007) 2191–95.
[42] MF Muldoon et al., *Arch Int Med* 155 (1995) 615–20.
[43] L Zgraggen et al., *Thromb Res* 115 (2005) 175–83.
[44] PD White et al., *Palaios* 13 (1998) 41–51.
[45] DE Fastovsky and A Bercovici, *Cretaceous Res* 57 (2016) 368–90.
[46] M Koupenova et al., *Europ Heart J* 38 (2017) 785–91.
[47] A Laurent and P Baumgart, *Bulletin de la Soc Mycol de France* 133 (2017) 143–57.
[48] M Monici, *Biotech Ann Rev* 11 (2005) 227–56.
[49] N Hoke et al., *Paleogeo Paleoclimatol Paleoecol* 310 (2011) 23–31.
[50] N Hoke et al., *Foren Sci Int* 228 (2013) 176.e1–176.e1766.
[51] TC Lee et al., *J Anat* 193 (Pt 2) (1998) 179–84.
[52] AID Prentice, *J Clin Path* 20 (1967) 717–19.
[53] F Ramsthaler et al., *Forensic Sci Int* 209 (2011) 59–63.
[54] MH Zheng et al., *Histochem J* 29 (1997) 639–43.
[55] DWE Hone et al., *PLoS ONE* 5 (2010) 1–7.
[56] A Nolte et al., *Handbook of Biological Confocal Microscopy*, 3rd ed., ed. JB Pawley, Springer Science and Business Media, New York, 2006, chapter 6, pp. 126–44.
[57] JM Starck and A Chinsamy, *J Morph* 254 (2002) 232–46.
[58] N Idris et al., *J Phys: Conf Ser* 846 (2015) 012020.
[59] L George et al., US Patent 6,592,882 (2003).
[60] Y Li et al., *Biol Fertil Soils* 39 (2004) 301–11.
[61] JM DeMassa and E Boudreaux, *Creation Res Soc Qtr* 51 (2015) 268–85.

MT